

Ultra-long, free-standing, single-crystalline vanadium dioxide micro/nanowires grown by simple thermal evaporation

Chun Cheng,^{1,2} Kai Liu,^{1,2} Bin Xiang,³ Joonki Suh,^{1,2} and Junqiao Wu^{1,2,a)}

¹Department of Materials Science and Engineering, University of California, Berkeley, California 94720, USA

²Materials Sciences Division, Lawrence Berkeley National Laboratory, Berkeley, California 94720, USA

³National Center for Electron Microscopy, Lawrence Berkeley National Laboratory, Berkeley, California 94720, USA

(Received 16 January 2012; accepted 21 February 2012; published online 9 March 2012)

Recently, it was discovered that single-crystalline VO₂ nanostructures exhibit unique, single-domain metal-insulator phase transition. They enable a wide range of device applications as well as discoveries of oxide physics beyond those can be achieved with VO₂ bulk or thin films. Previous syntheses of these nanostructures are limited in density, aspect ratio, single-crystallinity, or by substrate clamping. Here we break these limitations and synthesize ultra-long, ultra-dense, and free-standing VO₂ micro/nanowires using a simple vapor transport method. These are achieved by enhancing the VO₂ nucleation and growth rates using rough-surface quartz as the substrate and V₂O₅ powder as the evaporation source. © 2012 American Institute of Physics. [<http://dx.doi.org/10.1063/1.3693381>]

Vanadium dioxide (VO₂) is one of the most interesting materials due to its phase transition at a temperature slightly above room temperature ($T_C = 68^\circ\text{C}$). The first-order metal-insulator transition (MIT) is from the low-temperature, insulating, monoclinic phase to the high-temperature, metallic, tetragonal phase.¹ The transition features drastic changes in the lattice structure, electrical conductivity, and optical reflectivity. The transition could be exploited for device applications such as thermochromic coating, Mott transistors, and optical switches, as well as strain and gas sensors, but considerable challenges exist in engineering the MIT of VO₂ bulk or thin films for these applications. In particular, strain associated with grain boundaries, dislocations, stoichiometry fluctuation and substrate clamping causes the well-known issue of phase inhomogeneity, where a large number of metal and insulator domains co-exist in a wide range of temperatures.² This renders the phase transition broad and diffusive. In this regard, single-crystal VO₂ nanowires offer an appealing alternative because they host a single domain across their entire width, and thus support single- or few-domain MIT.^{3,4} Furthermore, from these VO₂ nanowires, aspects of the MIT physics are discovered,^{5,6} and device applications are demonstrated, such as actuators,⁷ sensors,⁸ power meters,⁹ and strain gauges.¹⁰

A variety of high-temperature synthesis methods for VO₂ micro/nanowires (MNWs) have been developed in recent years. In most of these syntheses, the as-grown VO₂ MNWs are embedded into the substrates with short lengths (typically less than 50 μm) and low densities. (This is because VO₂ wires cannot be grown using the standard, catalyzed vapor-liquid-solid method that allows growth of super-long, free-standing semiconductor nanowires.) Careful, selective etching is needed to release the VO₂ MNWs from the substrate in order to use them for the aforementioned de-

vice applications. This “liberation” process is typically slow, low-yield and may possibly damage the MNWs surface. It is, therefore, much needed to develop effective synthesis of single-crystal VO₂ MNWs at high densities, high aspect ratios that are also free-standing. Here we report the synthesis and characterization of ultra-long, ultra-dense, free-standing, single-crystalline VO₂ MNWs using a simple vapor transport method. V₂O₅ powder was placed in a quartz boat in the center of a horizontal tube furnace. The reaction product was collected on substrates downstream from the source quartz boat. The growth was carried out in the following condition: evaporation temperature ~880 °C, Ar carrier gas flow rate ~6.8 sccm, pressure ~5 Torr, evaporation time ~2 h or more. High-density growth of MNWs requires a careful choice of substrate surface: the greatest MNW density was achieved on rough (unpolished) surface of quartz substrate, while polished quartz and other species of substrates yield much lower densities of MNWs that were embedded in or strongly clamped on the substrates. The optimal deposition temperature is between 800 and 850 °C. The size distribution, lattice structure, and crystal orientation of the as-synthesized products were characterized by optical microscopy (CASCADE CMPS-888 L), scanning electron microscopy (SEM, Quanta 3D FEG), x-ray diffraction (XRD, Siemens D5000), and transmission electron microscopy (TEM, FEG CM200), as well as Raman spectroscopy (INVIA Raman Spectrometer with 488 nm Argon ion laser).

Figures 1(a) and 1(b) show representative optical images of the products. The reaction predominantly produces straight MNWs with ultra-long length in the range of 0.2-0.6 mm for microwires (deposition temperature 850 °C), or 0.1-0.3 mm for nanowires (deposition temperature 800 °C). Figure 1(c) and SEM images, such as that shown in the Fig. 1(a) inset, further indicate that these MNWs were grown free-standing from the substrate, which is in contrast to most previous growths.^{11,12} Figure 1(d) shows a representative XRD spectrum of an as-grown chip of MNWs and

^{a)}Author to whom correspondence should be addressed. Electronic mail: wuj@berkeley.edu.

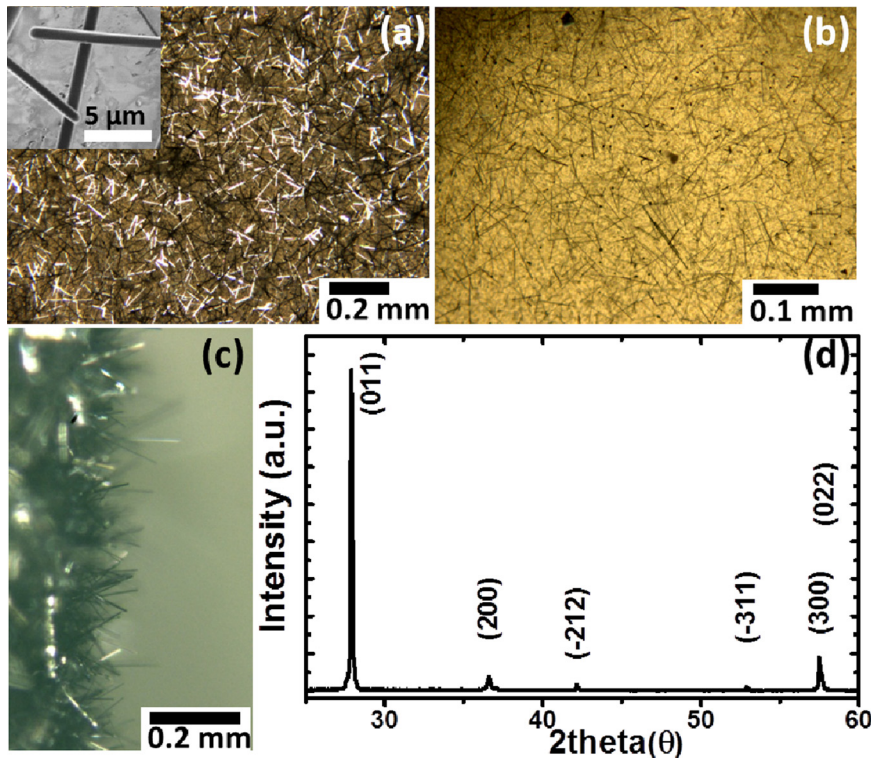


FIG. 1. (Color online) Optical images of products at deposition temperature of 850 °C (a) and 800 °C (b), respectively; Inset of (a): SEM image of as-grown VO₂ MNWs. (c) Optical image taken from the side view showing free standing. (d) XRD spectrum of the products.

demonstrates clearly that the produced MNW are crystalline. The XRD peaks can be indexed unambiguously to the low-temperature, monoclinic structure of VO₂ (JCPDS card 72-0514). It is noted that in addition to {0k1} peaks which appear in the in-plane growth of VO₂ MNWs,¹¹ there are also other peaks such as (200), (-212), (-311), (300), etc., suggesting randomly oriented free standing of the VO₂ MNWs and non-epitaxial growth on the quartz substrate.

The density and width of the wire products are sensitive to the deposition temperature. Figures 2(a) and 2(b) shows typical SEM images of products with deposition temperature

of 850 °C and 800 °C, respectively. It is apparent that the wire density is higher at higher deposition temperatures, estimated to be $> \sim 2 \times 10^9/\text{m}^2$ at 850 °C and $\sim 4 \times 10^8/\text{m}^2$ at 800 °C. The wire width distribution is shown in Fig. 2(c), indicating a broader distribution toward larger widths when the deposition temperature is higher. Figure 2(d) shows TEM image of a VO₂ nanowire and a selected area electron diffraction (SAED) pattern obtained from the nanowire. The nanowire has a smooth surface and a semi-round tip as growth front. The SAED pattern is indexed to be monoclinic VO₂. The diffraction spots were clear and round and the

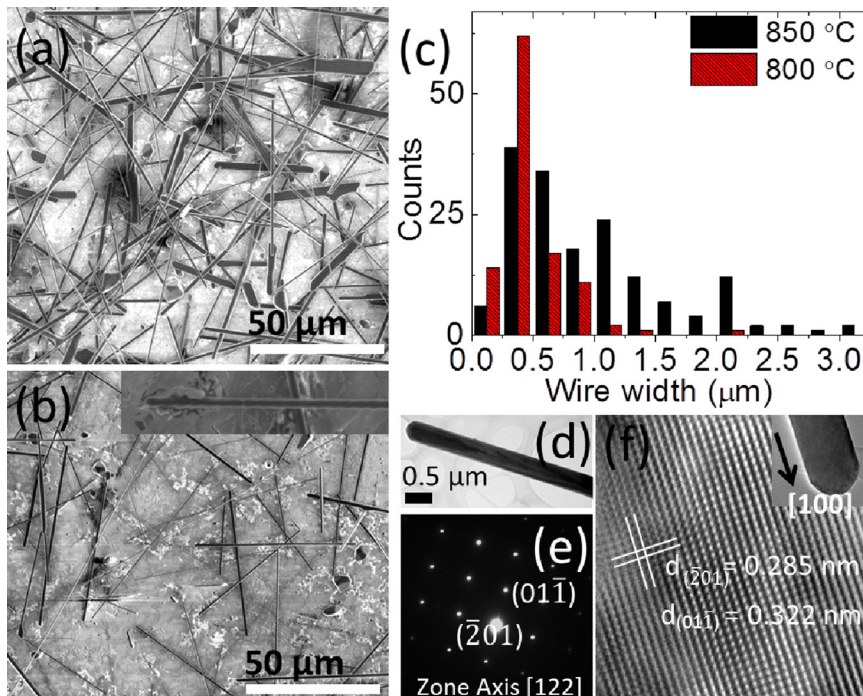


FIG. 2. (Color online) SEM images of products at deposition temperature of 850 °C (a) and 800 °C (b), respectively. Inset, an enlarged SEM image showing one MNW growing out of the surface; (c) Histogram of MNW widths measured from SEM images; (d) TEM image and (e) the corresponding SAED pattern of a single VO₂ MNW; (f) HRTEM image of a VO₂ MNW as shown in the Inset.

pattern did not change as the electron beam moved along the nanowire, indicating that the whole nanowire is a single crystal without stacking faults. Figure 2(f) shows a high-resolution TEM image of a nanowire with clear lattice fringes, again confirming good crystallinity of the nanowire. The marked lattice spacing of 0.285 nm and 0.322 nm corresponds to the inter-plane spacing of the (-201) and (01-1) planes of monoclinic VO₂ crystals, respectively. Careful analysis of the SAED patterns from multiple nanowires showed that the nanowires have axial growth plane of (-201) and, accordingly, a growth axis in the [100] direction (in the monoclinic coordinates).

In the case of long-time evaporation, ultra-long VO₂ fibers millimeters in length can be grown. Figure 3(a) shows a single, ultra-long VO₂ MNW transferred from the growth boat to a flat substrate. The MNW is 5.3 mm in length and has a uniform width of 2.2 μm along the entire MNW. It is noted that the surface of the MNW is smooth and clean and shows constant optical contrast, suggesting that this MNW is single crystalline as the shorter MNWs. Figure 3(b) shows optical images of the MIT of this VO₂ MNW under white light illumination; at low temperatures (27 °C) it is in the insulating phase (bright contrast), and it abruptly switches to the metallic phase (dark contrast) when temperature is above T_C; the contrast change occurs abruptly and uniformly for the whole MNW, indicating a uniform stoichiometry and strain-free nature of the MNW. Raman was used to determine the phase at temperatures below and above T_C as shown in Fig. 3(c). The Raman spectrum at room temperature shows characteristic vibration modes for the M1 insulating phase of VO₂. Comparing to previous work on thin film and bulk crystals, Raman peaks at room temperature are identified as 144(A_g), 192(A_g), 224(A_g), 260(B_g), 309(B_g), 392(A_g), 440(B_g), 497(A_g), 501(A_g), and 615(A_g) cm⁻¹.¹³ There are no peaks related to V₂O₅ and other stoichiometries, consistent with our XRD and TEM analyses. Above T_C, no Raman peaks were observed due to the metallicity of the MNW. The MIT in the VO₂ MNWs was studied by incorporating individual MNWs into a four-probe geometry

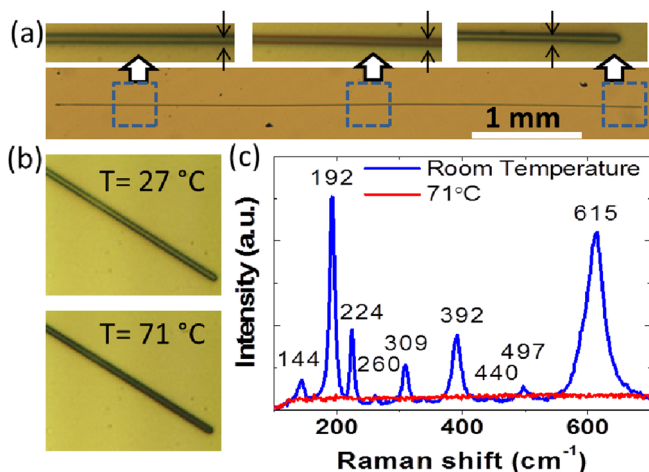


FIG. 3. (Color online) (a) Optical image of a 5-millimeter-long VO₂ MNW; (insets) magnified images of the MNW at selected areas. (b) Optical images of this MNW at room temperature (27 °C, insulating phase) and a temperature above T_C (71 °C, metallic phase); (c) Raman spectra taken from this MNW before and after the MIT.

using electron-beam lithography and measuring their resistance (*R*) as a function of temperature (*T*).³ The four contacts were formed by bonding the MNW onto the pre-deposited Au electrodes with depositing Pt using a focused ion beam. The I-V of the thus-fabricated devices was linear, indicating ohmic contacts. Figure 4(a) shows the four-probe *R* versus *T* of four devices that were cut from one single millimeter-long MNW. These four devices show nearly the same resistance behavior, switching from several MΩ to tens of Ω upon the MIT. The exact MIT temperature and its hysteresis vary between devices, which is a well known effect and caused by the sensitivity of MIT to the axial or flexural strain in such an end-clamping MNW.³ It can be envisioned that these ultra-long MNWs with uniform properties can be aligned, positioned and integrated into large-scale systems for functional device applications.¹⁴

The thermal evaporation method to synthesize VO₂ MNWs was first developed by Guiton *et al.*, in which VO₂ powder was thermally evaporated onto flat silicon, quartz, oxidized silicon surface, or sapphire etc.¹¹ The growth of VO₂ MNWs by thermal evaporation was considered as a vapor-solid (VS) mechanism, with vanadium oxides undergoing evaporation and/or decomposition to various vanadium oxides at temperatures above 700 °C. The oxide vapor is carried downstream by the carrier gas, and the stable VO₂ phase nucleates from the precursor and grows on the substrates. The thus-obtained VO₂ MNWs are very sparse and always embedded into or clamped onto the substrates due to high affinity between the precursor droplets and these substrates. The length of MNWs is also quite short and limited to ~50 μm. V₂O₅ has also been used as the evaporated

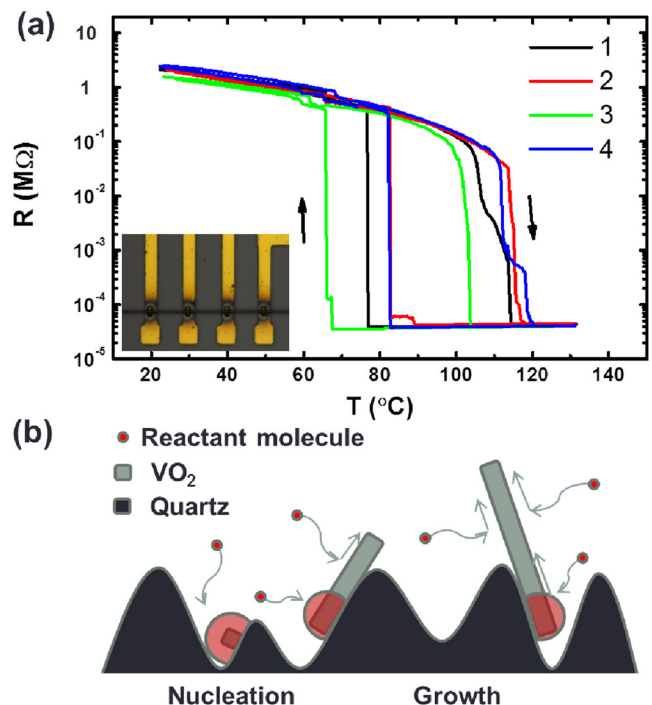


FIG. 4. (Color online) (a) Temperature dependent resistance (*R*(*T*)) curves of four VO₂ devices, each of which was made from a MNW cut from a single mm-long VO₂ MNW. Inset, optical image of a four-probe VO₂ MNW device (Pt was used to bond the MNW onto the underlying electrodes); (b) Proposed growth mechanism of free-standing VO₂ MNWs on rough quartz substrates.

reactant for the growth of VO₂ MNWs,^{14,15} because it has a much lower melting point of 690 °C than that of VO₂ (1967 °C), hence can provide much higher vapor pressure and should enhance the VO₂ growth. However, the VO₂ MNWs grown using V₂O₅ powder are still short (<~30 μm) (Ref. 15) or sparse.¹⁶ Our work demonstrates that a special type of substrates, unpolished (rough) quartz, facilitates growth of MNWs at high densities, large lengths, and free standing. Strelcov *et al.*¹⁶ studied the in situ growth process of VO₂ nanostructures from thermal evaporation of V₂O₅. They proposed a wetting layer assisted growth mechanism: VO₂ nanowire growth occurs at the developing apex of the nanowires with the feeding materials supplied via the peripheral liquid wetting layer (V₂O₅). Capillary forces induced by the liquid wetting on the smooth substrate surface result in exclusively in-plane nanowire growth. Our MNW growth follows the same growth mechanism because of similar reaction process, except that the surface of quartz is rough in our case. The free-standing growth as shown in Figs. 1(c) and 2(b) is enabled by the rough surface and can be explained in Fig. 4(b). When the VO₂ nucleates and grows out of a V₂O₅ droplet, owing to the capillary forces, the initial VO₂ MNWs are bound onto the local surface plane. However, at later times, following the surface roughness, the growth front grows out the plane and becomes free-standing (Fig. 4(b)). This explains the random orientation of the as-grown MNWs in Fig. 1(c). In additional, compared to MNWs grown embedded in substrates, the free-standing MNWs allow more surface of wires exposed to the gas reactant. Therefore more reactant molecules can be adsorbed and diffuse to the growth front, resulting in a faster and free-standing lateral and axial growth. In contrast, in previous methods of growing VO₂ MNWs embedded into the substrate surface, the growth front has to constantly overcome obstructions from the substrate chemistry and morphology, resulting in limited length or non-uniform diameter of the MNWs. This explains the capability of this present method to grow ultra-long, straight, and single-crystalline VO₂ MNWs with uniform diameter and stoichiometry. We found that combination with V₂O₅ evaporation source improved the VO₂ nucleation and led to an even faster, denser growth of free-standing VO₂ MNWs. Under the same reaction conditions, we found nearly no free-standing wire growth when silicon or sapphire substrates were used, no matter they are polished or unpol-

ished. The sensitivity of growth behavior to the surface roughness and chemical identity of substrates suggests that the rough quartz surface provides the best seeding environment.

In summary, single-crystalline, free-standing, ultra-long (>several mm), and ultra-dense (>10⁹/m²) VO₂ micro/nanowires have been synthesized by a simple thermal evaporation method. Combination of using low-melting-point source V₂O₅ and rough quartz substrates greatly facilitates nucleation and enhances the growth rate. These free-standing VO₂ MNWs can be easily harvested and transferred to substrates, which enable studies of domain physics of the phase transition, as well as integrated device applications such as power gauges, gas sensors, actuators, memories, and optical switches.²

This work is financially supported by the National Science Foundation Nano-scale Science and Engineering Center (NSF-NSEC) for Scalable and Integrated NANOManufacturing (SINAM) (Grant No. CMMI-0751621). The materials characterization part was supported by the NSF under Grant No. CMMI-1000176.

¹V. Eyert, *Ann Phys. (Berlin, Ger.)* **11**, 650 (2002).

²J. Cao and J. Wu, *Mater. Sci. Eng. R* **71**, 35 (2011).

³J. Wu, Q. Gu, B. S. Guiton, N. P. de Leon, L. Ouyang, and H. Park, *Nano Lett.* **6**, 2313 (2006).

⁴J. Cao, E. Ertekin, V. Srinivasan, W. Fan, S. Huang, H. Zheng, J. W. L. Yim, D. R. Khanal, D. F. Ogletree, J. C. Grossman, and J. Wu, *Nat. Nanotechnol.* **4**, 732 (2009).

⁵J. Wei, Z. Wang, W. Chen, and D. H. Cobden, *Nat. Nanotechnol.* **4**, 420 (2009).

⁶J. Cao, W. Fan, K. Chen, N. Tamura, M. Kunz, V. Eyert, and J. Wu, *Phys. Rev. B* **82**, 241101 (2010).

⁷Y. Gu, J. Cao, J. Wu, and L.-Q. Chen, *J. Appl. Phys.* **108**, 083517 (2010).

⁸E. Strelcov, Y. Lilach, and A. Kolmakov, *Nano Lett.* **9**, 2322 (2009).

⁹C. Cheng, W. Fan, J. Cao, S.-G. Ryu, J. Ji, C. P. Grigoropoulos, and J. Wu, *ACS Nano* **5**, 10102 (2011).

¹⁰B. Hu, Y. Ding, W. Chen, D. Kulkarni, Y. Shen, V. V. Tsukruk, and Z. L. Wang, *Adv. Mater.* **22**, 5134 (2010).

¹¹B. S. Guiton, Q. Gu, A. L. Prieto, M. S. Gudixsen, and H. Park, *J. Am. Chem. Soc.* **127**, 498 (2005).

¹²S. Zhang, I. S. Kim, and L. J. Lauhon, *Nano Lett.* **11**, 1443 (2011).

¹³C. Xiang-Bai, *J. Korean Phys. Soc.* **58**, 100 (2011).

¹⁴M. Yaman, T. Khudiyev, E. Ozgur, M. Kanik, O. Aktas, E. O. Ozgur, H. Deniz, E. Korkut, and M. Bayindir, *Nat. Mater.* **10**, 494 (2011).

¹⁵B. Varghese, R. Tamang, E. S. Tok, S. G. Mhaisalkar, and C. H. Sow, *J. Phys. Chem. C* **114**, 15149 (2010).

¹⁶E. Strelcov, A. V. Davydov, U. Lanke, C. Watts, and A. Kolmakov, *ACS Nano* **5**, 3373 (2011).